Effect of NaOH concentration on structural, surface and antibacterial activity of CuO nanorods synthesized by…

Article *in* Superlattices and Microstructures · February 2014

DOI: 10.1016/j.spmi.2013.10.020

6 authors, including:

Sonia S
Holy Cross College (Autonom…
8 PUBLICATIONS **34** CITATIONS
SEE PROFILE

Ponpandian Nagamony
Bharathiar University
114 PUBLICATIONS **2,292** CITATIONS
SEE PROFILE

Superlattices and Microstructures 66 (2014) 1–9

Contents lists available at ScienceDirect

Superlattices and Microstructures

journal homepage: www.elsevier.com/locate/superlattices

Effect of NaOH concentration on structural, surface and antibacterial activity of CuO nanorods synthesized by direct sonochemical method

S. Sonia [a], Naidu Dhanpal Jayram [a], P. Suresh Kumar [b], D. Mangalaraj [a,*], N. Ponpandian [a], C. Viswanathan [a]

[a] Department of Nanoscience and Technology, Bharathiar University, Coimbatore 641 046, India
[b] Thin Film and Nanomaterials Laboratory, Department of Physics, Bharathiar University, Coimbatore 641 046, India

ARTICLE INFO

Article history:
Received 9 July 2013
Received in revised form 2 October 2013
Accepted 12 October 2013
Available online 25 November 2013

Keywords:
CuO
Nanorods
Sonochemical
Optical properties
Antibacterial activity

ABSTRACT

Highly efficient Copper oxide (CuO) nanorods were synthesized by using one step sonochemical method under room temperature with change in NaOH concentration. XRD confirms the prepared nanorods are in pure monoclinic phase with lattice constants $a = 4.68$ Å, $b = 3.42$ Å, and $c = 5.13$ Å and FESEM analysis reveals an average diameter of 50–100 nm. Optical absorption spectra exhibits the strong blue shift compared with bulk and the bandgap increases with decreasing the size of the nanorods which is due to the nanosize effect. The composition of CuO nanorods were characterized by Fourier Transform Infra-Red spectroscopy (FTIR) which confirms the formation of monoclinic phase of CuO and the Thermal analysis was done by Thermo Gravimetric Analysis (TGA). The antibacterial properties of copper oxide nanorods were investigated using human pathogens and was compared based on diameter of inhibition zone using agar well diffusion method. The synthesized copper oxide nanostructures show excellent antibacterial activity against *Salmonella typhimurium* than *Staphylococcus aureus* strain.

* Corresponding author. Tel.: +91 422 2425458; fax: +91 422 2422387.
E-mail address: dmraj800@yahoo.com (D. Mangalaraj).

0749-6036/$ - see front matter © 2013 Elsevier Ltd. All rights reserved.
http://dx.doi.org/10.1016/j.spmi.2013.10.020

1. Introduction

Copper oxide (CuO) has attracted much attention in recent years because of its promising applications such as solar cells, gas sensors, and superconductors [1–3]. Cupric Oxide having monoclinic structure is a unique monoxide compound for both fundamental investigations and practical applications. Being a p-type covalent semiconductor, CuO reveal a narrow band gap between 1.2 and 1.5 eV, this makes it an ideal choice for alternative materials to serve as field emitters. CuO is a key component in high T_c superconductors and is also used as a photoconductive material. Owing to its photochemical properties, CuO has been widely used in the fabrication of anode material for Li-ion battery [4,5]. Only limited information on its inactivation of bacteria has been reported up-till now [6–10]. It has been realized that CuO is an effective antimicrobial agent owing to its ionization property and is cost effective when compared with silver and easily mixes up with polymers and is relatively chemically stable. The large surface area and easy formation of various morphologies (such as microspheres [12], nanoflowers [11], nanoleaves [13], of CuO bestow excellent antibacterial activity.

Bacterial strains, such as *Salmonella typhimurium* and *Staphylococcus aureus* have the ability to cause gastroenteritis and skin infections and it is difficult to recognize. Hospitals and transport are two particular areas that offer opportunities for the use of nanoparticulate metals and metal oxides to prevent the spread of infection. With the increase in transportation facilities, people are exposed to more airborne, vector-borne and zoonotic spread of infectious agents [14]. Therefore, in terms of potential use the incorporation of nanoparticulate metals and metal oxides into surfaces and other objects could be envisaged. CuO nanoparticles also have adverse effects on bacteria, and Cu^{2+} dissolving from CuO NPs induced toxic effects by triggering ROS production and DNA damage in bacteria [15]. The method for the synthesis of nanomaterials is considered to be one of the most important criteria for obtaining high efficiency, excellent potential and high-quality product. Owing to their wide scope, various nanostructures of CuO have been synthesized by various techniques such as hydrothermal [16], electrochemical deposition [11], Reflux condensation [9], and chemical bath deposition [13]. All the above methods need high temperature to obtain different morphologies. When compared with the above techniques discussed, sonochemical method is the most viable and better option because homogenously dispersed nanostructures induced by ultrasonic cavitation [17]. In this present work, a simple sonochemical method is employed to synthesize CuO nanorods at room temperature with copper acetate and sodium hydroxide as starting materials. Without using any surfactants or templates CuO nanorods were obtained by tuning the concentrations of the reactants in the solution. In addition, the antibacterial activity against *S. typhimurium* and *S. aureus* strains of the as prepared CuO nanorods is studied.

2. Experimental procedure

2.1. Synthesis of CuO nanorods

CuO nanorods were prepared by simple sonochemical method. In a typical reaction process, 25 ml of 0.5 M aqueous solution of NaOH was mixed slowly in 50 ml of 0.2 M aqueous solution of copper acetate dihydrate under continuous stirring for 30 min. The resultant solutions were then sonicated for 2 h at room temperature and the pH was maintained at 12. Finally the black colored precipitate obtained was washed with distilled water and ethanol several times and dried at 80 °C for 2 h. Similar reactions were also carried out for 0.5 M, 1.0 M, 1.5 M, 2.0 M NaOH concentrations. The reaction mechanism for the formation of cupric oxide is as follows:

$$Cu(CH_3COO)_2 + NaOH \rightarrow Cu(OH)_2 + CH_3COONa \rightarrow CuO + H_2O$$

The concentration of NaOH plays a vital role for the formation of CuO nanorods since OH^- is strongly related to the reaction that produces nanostructures. The separated colloidal Cu $(OH)_2$ clusters in solution acts partly as nuclei for the growth of CuO nanorods. During the sonochemical growth process, the Cu $(OH)_2$ dissolves under ultrasonic radiation at room temperature. When the concentrations of Cu^{2+} and OH^- reach the critical value of the supersaturation, fine CuO nuclei form spontaneously in the

aqueous complex solution and CuO nanoparticles combine together to reduce the interfacial free energy. This is because the molecules at the surface are energetically less stable than the ones already well ordered and packed in the interior. Incorporation of growth units into crystal lattice of the nanorods by dehydration reaction takes place. It was concluded that the growth habit was determined by thermodynamic factor and by concentration of OH^- as the kinetic factor in aqueous solution growth.

2.2. Antibacterial activity

Antimicrobial activities of the as-synthesized copper oxide nanostructures were performed against *S. typhimurium* and *S. aureus*. Bacterial sensitivity of copper oxide nanostructures are tested using agar-well diffusion method. The bacterial suspension was applied uniformly on the surface of Luria bertani agar plate and agar-wells were punched using agar punches. Then, synthesized CuO nanoparticles were added in the 25 μg/L concentration. The plates were incubated at 35 °C for 24 h, after which the average diameter of the inhibition zone surrounding the disk was measured with a ruler up to 1 mm resolution.

2.3. Characterization techniques

A PAN analytical (XPERT-PRO) X-ray diffractometer using Cu $K\alpha_1$ radiation (λ = 1.5406 Å) was employed to characterize the crystallographic properties of the CuO nanorods. The surface morphologies were characterized by a FEI Quanta-250 Field Emission Scanning Electron Microscopy (FESEM). UV–Vis spectral analysis was recorded on Jasco V-650 Spectrophotometer. FT-IR analysis was performed by Bruker Tensor 27, Fourier Transforms Infrared spectroscope. Thermal analysis was done by Perkin Elmer-Diamond Thermo Gravimetric Analysis (TGA).

3. Results and discussion

3.1. Structural and surface analysis

By adjusting the concentration of sodium hydroxide (NaOH), CuO nanorod structures have been prepared via an aqueous sonochemical route under ambient temperature. The powder XRD pattern of CuO nanorods synthesized at different reaction conditions are shown in Fig. 1. The result shows the presence of good crystalline material and is well indexed to infer to be monoclinic phase when compared with bulk material (JCPDS 05-0661) with lattice constants a = 4.68 Å, b = 3.42 Å and c = 5.13 Å. The major peaks located at 2θ = 35.43° and 38.49° are indexed as (0 0 2) and (1 1 1) planes respectively and are the characteristics peaks for the pure phase monoclinic CuO nanoparticles (Fig. 1a–c). The sharp and narrow diffraction peaks indicate that the material has good crystallinity. No characteristic peaks from the intermediates such as Cu $(OH)_2$ was detected. The average grain size of copper oxide nanorods is calculated by using the Scherrer formula ($D = 0.89\lambda/\beta\cos\theta$). where D is the crystallite size, λ is the wavelength (1.5406 Å for Cu Kα), β is the full-width at half-maximum (FWHM) of main intensity peak after subtraction of the equipment broadening and θ is the diffraction angle. The average grain size was found to be around 20–35 nm for CuO nanorods.

The crystallite size of the nanorods also compared with the Williamson–Hall plot (W–H plot). The instrumental broadening (β_{hkl}) was corrected, corresponding to each diffraction peak of CuO nanorods using the relation:

$$\beta_{hkl} = \left[(\beta_{hkl})^2_{Measured} - (\beta_{hkl})^2_{Instrumental}\right]^{1/2} \quad (1)$$

Williamson and Hall proposed a method for calculating the size and strain broadening by looking at the peak width as a function of diffracting angle 2θ and obtained an expression [18].

$$\beta_{hkl}\cos\theta = \frac{K\lambda}{D} + 4\varepsilon\sin\theta \quad (2)$$

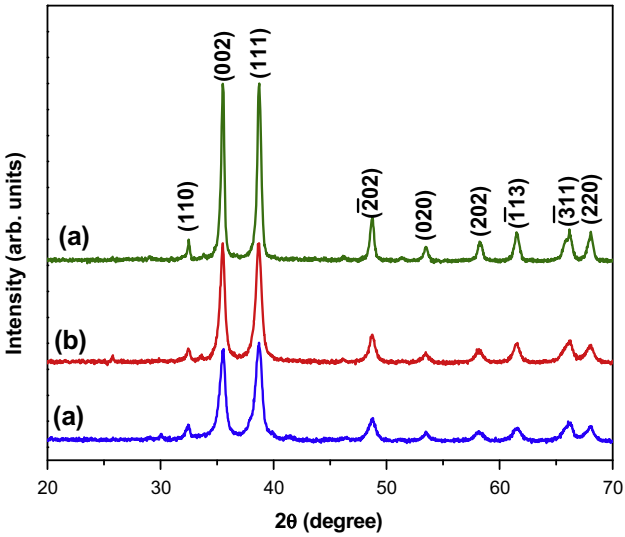

Fig. 1. XRD spectra of CuO nanorods prepared at different molar concentration of NaOH at (a) 1.0 M (b) 1.5 M and (c) 2.0 M.

A plot is drawn for 4 sin θ along the *X*-axis and β_{hkl} cos θ along the *Y*-axis for prepared CuO nanorods and is shown in Fig. 2. The crystallite size (~19–34 nm) is calculated from the *y*-intercept of the linear fit and is consistent with the crystallite size calculated from the Scherrer formula. Fig. 3(a–d) displays FESEM images of CuO nanorods grown at room temperature with the NaOH concentration of 0.5 M, 1.0 M, 1.5 M and 2.0 M. The morphology of CuO sample grown at 0.5 M NaOH (Fig. 3a) shows the initial formation of CuO nanorods and is typically about 250–500 nm in length and 50–100 nm in

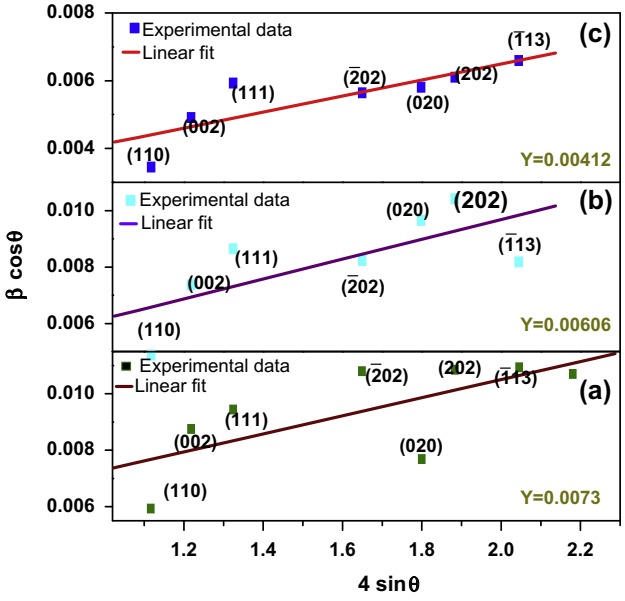

Fig. 2. W–H plot of CuO nanorods prepared at different molar concentration of NaOH at (a) 1.0 M (b) 1.5 M and (c) 2.0 M.

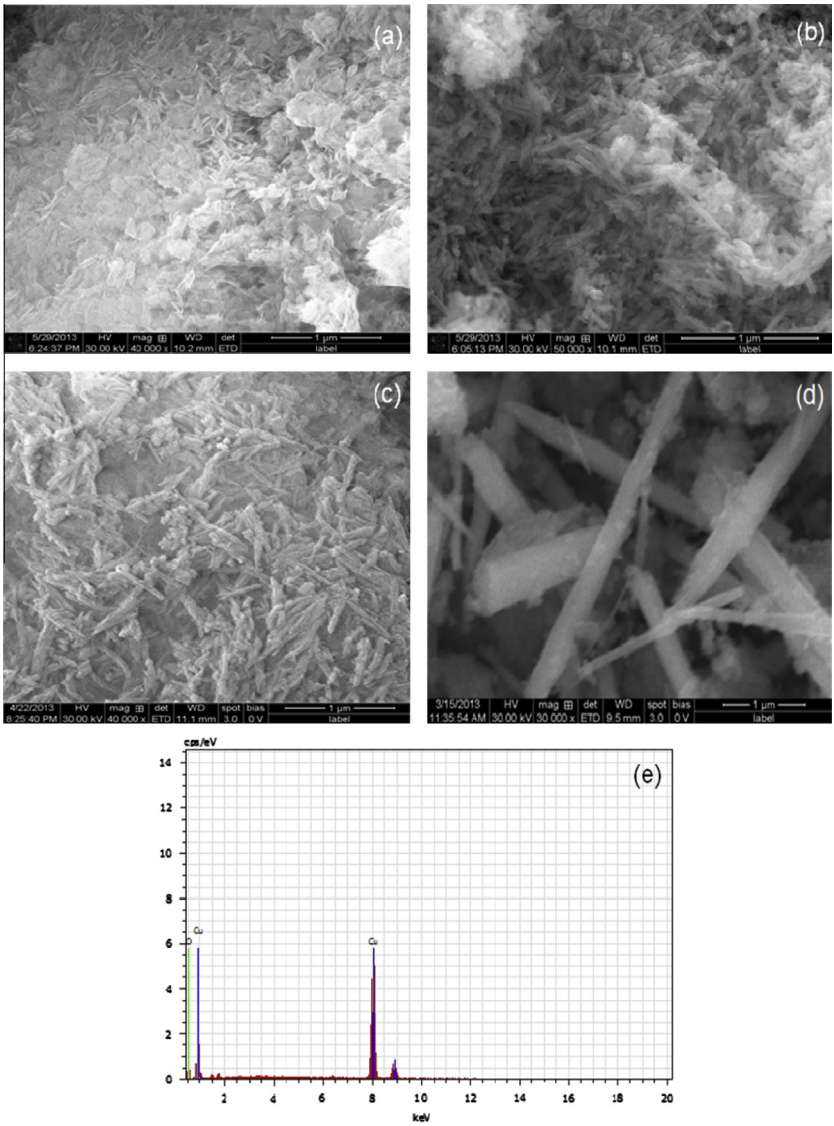

Fig. 3. Fesem images of CuO nanorods prepared at different molar concentration of NaOH at (a) 0.5 M (b) 1.0 M (c) 1.5 M (d) 2.0 M and (e) energy-dispersive X-ray (EDX) spectra of CuO nanorods.

diameter. Fig. 3(b and c) shows the morphology of nanorods grown at 1.0 M and 1.5 M NaOH under the same conditions and the nanorods are observed as aggregation. These CuO nanorods show an average diameter of 100 nm and length of 500–750 nm. When the synthesis process was carried out at higher concentration of NaOH (0.2 M) individual CuO nanorods were obtained (Fig. 3d) and the average diameter is 250 nm. High concentration of NaOH and the consequent pH of the reaction mixture decide the morphology of the nanorods. The complex ion in the reaction mixture is converted to Cu $(OH)_2$ which then decomposes to form CuO nanorods [19]. We found that through optimization of the Cu^{2+}/OH^{-} concentrations, CuO nanorods can be obtained. When the concentration of NaOH to Cu $(CH_3COO)_2$ ratio increases the thickness of the nanorods also gets increased as shown in Fig. 3d.

This was explained by the increase of the amount of OH^- ions produced from higher concentration of NaOH [20]. Through our experiments, we systemically studied the influence of NaOH concentration on the morphology of the CuO nanorods. The result shows that the size of nanorods is strongly dependent on NaOH concentration. Fig. 3 shows that the width of the nanorods diminishes when decreasing the concentration by keeping all other parameters constant. Our results show that controlled growth of nanorods ranging from a thinner to a larger diameter can be realized by appropriate choice of the NaOH concentration. EDAX pattern of CuO (Fig. 3e) shows sharp peaks corresponding to Cu (K) and O (K). The Cu:O composition was found to be 57.06:42.94 confirming its high purity.

3.2. Optical properties and thermal analysis

The absorption spectra of the as-synthesized samples at 0.5 M, 1.0 M, 1.5 M and 2.0 M of NaOH concentration is shown in Fig. 4 and their broad absorption peaks are observed at 354.59, 358.01, 360.9 and 367.4 nm, respectively. The optical band gap of the material is obtained by using the following equation [21].

$$\alpha h\nu = K(h\nu - E_g)^m \tag{3}$$

where α is the absorbance, K is a constant, and m equals 1 for direct transition and 2 for indirect transition. Inset of Fig. 4 show a plot of $(\alpha h\nu)^2$ versus $h\nu$ plot for direct transition, and the extrapolation of linear curve to zero absorption edge energy corresponds to band gap E_g. The band gap of as-obtained CuO is estimated to be 3.09 eV, which shows a greater blue-shift compared with that of the bulk (1.2 eV) due to quantum size effect [22].

Essentially, the optical properties of nanoparticles are determined by their energy band. The size of the nanorods synthesized using 0.5 M, 1.0 M and 1.5 M NaOH is smaller than that of the nanorods synthesized using 2.0 M NaOH which leads to stronger quantum confinement effect. Thus, the absorption peak of the nanorods at 0.5 M has a larger "blue shift" than that of the nanorods at 1.0 M, 1.5 M and 2.0 M. Therefore, our studies show that the optical properties of nanostructures could be adjusted by change in size of nanorods.

The composition and quality of the CuO nanorods were analyzed by FTIR, in the range of 400–4000 cm^{-1} (Fig. 5). The absorption bands at 430, 507, and 606 cm^{-1} have been observed from the FTIR

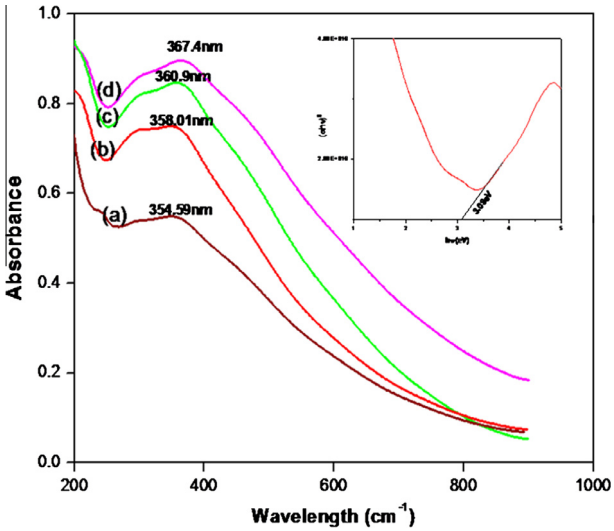

Fig. 4. Absorption spectra of CuO nanorods prepared at different molar concentration of NaOH at (a) 0.5 M (b) 1.0 M (c) 1.5 M and (d) 2.0 M. Inset figure shows the plot of $(\alpha h\nu)^2$ versus $h\nu$.

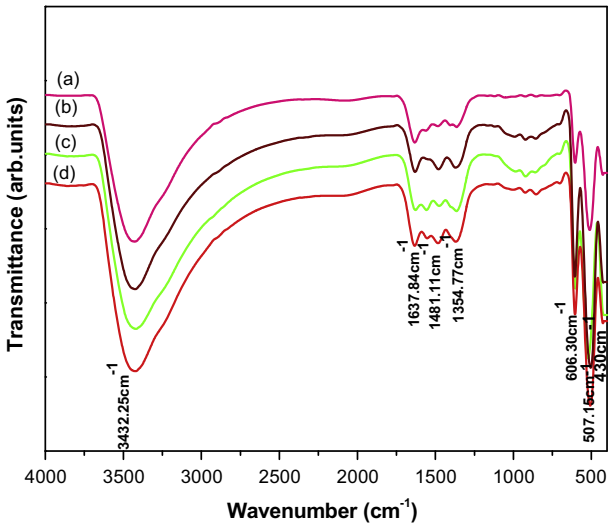

Fig. 5. FTIR spectra of CuO nanorods prepared at different molar concentration of NaOH at (a) 0.5 M (b) 1.0 M (c) 1.5 M and (d) 2.0 M.

spectrum which is due to the Cu–O stretching in the monoclinic phase of CuO [23]. Weak and broad absorption bands at 1637 and 3432 cm^{-1} have been observed due to the existence of water molecules and 1354 cm^{-1} is due to C–H stretching vibrations. The TGA test of the CuO nanorods was conducted simultaneously at a heating rate of 20 °C/min from 50 °C to 700 °C and air is used as purged gas in the analysis, the result is shown in Fig. 6 According to the result, there was no notable decomposition in the TGA curve is observed and the gradual weight loss has been noted from 250 °C proving the stability of CuO is high.

3.3. Antibacterial analysis

Fig. 7(a–d) presents the zone of inhibition of nanorods against the Bacterial strains *S. typhimurium* and *S. aureus*. All the samples show the effective bacterial retardant behavior. However nanorods prepared at 2.0 M NaOH concentration showed excellent antibacterial activity than other samples as shown in Fig. 7d. This indicates that the morphology or the dimensionality of Nanomaterials can immensely affect the antibacterial activity. Since, the different surface-interface characteristics might

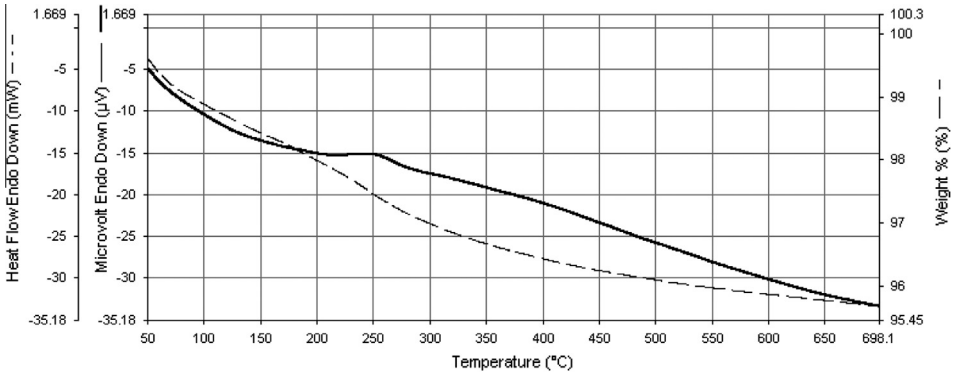

Fig. 6. TGA/DTA curve of CuO nanorods prepared at molar concentration of NaOH at 2.0 M.

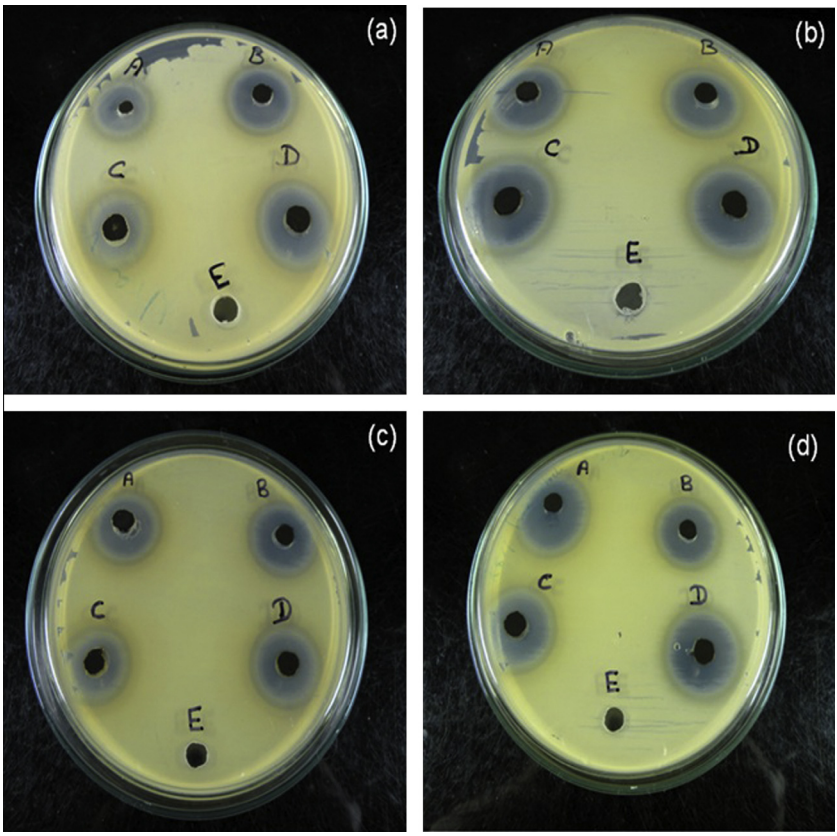

Fig. 7. Zone of inhibition of the CuO nanostructures with minimum inhibitory concentration of 25 μg/L for (a) *Staphylococcus aureus* (b) *Salmonella typhimurium* and zone of inhibition of the nanostructures with maximum inhibitory concentration of 100 μg/L for (c) *Staphylococcus aureus* and (d) *Salmonella typhimurium*. (*Note*: A-0.5 M NaOH; B-1.0 M NaOH; C-1.5 M NaOH; D-2.0 M NaOH; E-Control (water).

Table 1
Zone of inhibition of CuO nanorods against *Staphylococcus aureus* and *Salmonella typhimurium*.

Samples code	Zone of inhibition (mm)			
	Salmonella typhimurium		*Staphylococcus aureous*	
	(25 μl/l)	(100 μl/l)	(25 μl/l)	(100 μl/l)
A-0.5 M NaOH	20	20	12	18
B-1.0 M NaOH	21	20	20	17
C-1.5 M NaOH	21	21	19	18
D-2.0 M NaOH	22	22	20	19
E-Control (water)	–	–	–	–

have different chemical–physical adsorption–desorption abilities towards the bacteria, ensuing in different antibacterial activities [19]. From Fig. 7 the zone of inhibition measured are listed in Table 1. Interaction between the nanoparticles and the cell wall of bacteria congeries the fact that the growth of *S. typhimurium* was more effectively affected by CuO nanostructures than that of the *S. aureus*

bacteria. Several studies have been suggested that, the two possible mechanisms could be involved in the interaction between nanoparticles and bacteria: (1) the production of increased levels of reactive oxygen species (ROS), mostly hydroxyl radicals and singlet oxygen [21,24] and (2) deposition of the nanoparticles on the surface of bacteria or accumulation of nanoparticles either in the cytoplasm or in the periplasmic region causing disruption of cellular function and/or disruption and disorganization of membranes [25]. Reactive oxygen species (ROS), such as hydrogen peroxide (H_2O_2), superoxide anion ($O_2^{\cdot-}$), hydroxyl radicals (OH_3), and organic hydro peroxides (OHPs) are toxic to the cells as they damage cellular constituents such as DNA, lipids, and proteins [26]. The antibacterial activity of CuO towards Gram-negative bacteria was higher when compared to Gram-positive bacteria. The difference in activity against these two types of bacteria could be attributed to the structural and compositional differences of the cell membrane [27]. Gram-positive bacteria have thicker peptidoglycan cell membranes compared to the Gram-negative bacteria and it is harder for CuO to penetrate it, resulting in a low antibacterial response [11]. The antibacterial effect was detected due to the CuO nanoparticles, which can generate reactive oxygen species that are responsible for damaging the bacteria's cells.

4. Conclusion

In summary, we have proposed a simple Sonochemical Approach at room temperature for the fabrication of CuO nanorods without any surfactants and templates. The results shows that the variation in the concentration of NaOH have influence the morphology of CuO nanorods. The influence of chemical reactions, nucleation and growth process on the morphology of CuO nanorods are discussed. Our experimental results demonstrated that the as-prepared CuO nanorods exhibited very effective antibacterial activity against *S. typhimurium* than *S. aureus* strain and can easily inhibit the bacterial growth at the concentration of 25 μg/mL. The result suggest that CuO nanoparticles have a potential application as a bacteriostatic agent and may have future applications in the development of derivative agents to control the spread and infection of variety of bacterial strains.

References

[1] R. Sahay, J. Sundaramurthy, P.S. Kumar, V. Thavasi, S.G. Mhaisalkar, S. Ramakrishna, J. Solid State Chem. 186 (2012) 261–267.
[2] S. Gao, S. Yang, J. Shu, S. Zhang, Z. Li, K. Jiang, J. Phys. Chem. C 112 (2008) 19324–19328.
[3] A. Comanac, L.D. Medici, M. Capone, A.J. Millis, Nat. Phys. 4 (2008) 287–290.
[4] R. Sahay, P.S. Kumar, V. Aravindan, J. Sundaramurthy, W.C. Ling, S.G. Mhaisalkar, S. Ramakrishna, S. Madhavi, J. Phys. Chem. C 116 (2012) 18087–18092.
[5] Y. Liu, L. Zhong, Z. Peng, Y. Song, W. Chen, J. Mater. Sci. 45 (2010) 3791–3796.
[6] R. Sathyamoorthy, K. Mageshwari, Physica E 47 (2013) 157–161.
[7] L. Lu, X. Huang, Microchim. Acta 175 (2011) 151–157.
[8] P. Pandey, S. Merwyn, G.S. Agarwal, B.K. Tripathi, S.C. Pant, J. Nanopart. Res. 14 (2012) 709–721.
[9] I. Perelshtein, G. Applerot, N. Perkas, E. Wehrschuetz-Sigl, A. Hasmann, G. Guebitz, A. Gedanken, Surf. Coat. Technol. 204 (2009) 54–57.
[10] R. Wahab, S.T. Khan, S. Dwivedi, M. Ahamed, J. Musarrat, A.A. Al-Khedhairy, Colloids Surf. B 111 (2013) 211–217.
[11] Y. Zhao, J. Zhao, Y. Li, D. Ma, S. Hou, L. Li, X. Hao, Z. Wang, Nanotechnology 22 (2011) 115604–115609.
[12] N. Hanagata, M. Xu, T. Takemura, F. Zhuang, Nano Biomed. 2 (2010) 153–169.
[13] N. Ekthammathat, T. Thongtem, S. Thongtem, Appl. Surf. Sci. 277 (2013) 211–217.
[14] Y. Fan, R. Liu, W. Du, Q. Lu, H. Pang, F. Gao, J. Mater. Chem. 22 (2012) 12609–12617.
[15] S. Zaman, M.H. Asif, A. Zainelabdin, G. Amin, O. Nur, M. Willander, J. Electroanal. Chem. 662 (2011) 421–425.
[16] S.J. Putterman, K.R. Weninger, Ann. Rev. Fluid Mech. 32 (2000) 445–476.
[17] A.Y. Baranchikov, V.K. Ivanov, Y.D. Tretyakov, Russ. Chem. Rev. 76 (2007) 133–151.
[18] R.B. Kale, Y.J. Hsu, Y.F. Lin, S.Y. Lu, Solid State Commun. 142 (2007) 302–305.
[19] H. Zhang, D. Yang, Y.J. Yi, X.Y. Ma, J. Xu, D.L. Que, J. Phys. Chem. B 108 (2004) 3955–3963.
[20] O. Krichershy, J. Stavan, Phys. Rev. Lett. 70 (1993) 1473–1479.
[21] H. Yang, C. Liu, D. Yang, H. Zhang, Z. Xi, J. Appl. Toxicol. 29 (2009) 69–78.
[22] B. Subramanian, C. Sanjeeviraja, M. Jayachandran, J. Cryst. Growth 234 (2002) 421–426.
[23] G. Zou, H. Li, D. Zhang, K. Xiong, C. Dong, Y. Qian, J. Phys. Chem. B 110 (2006) 1632–1637.
[24] L. Zhang, Y. Jiang, Y. Ding, M. Povey, D. York, J. Nanopart. Res. 9 (2007) 479–489.
[25] G. Storz, J.A. Imlay, Curr. Opin. Microbiol. 2 (1999) 188–194.
[26] M. Heinlaan, A. Ivask, I. Blinova, H.C. Dubourguier, A. Kakru, Chemosphere 71 (2008) 1308–1316.
[27] J.S. Tawale, K. Dey, R. Pasricha, K.N. Sood, A.K. Srivastava, Thin Solid Films 519 (2010) 1244–1247.